Article

Experimental Study about Shale Acceleration on Methane Cracking

Jingkui Mi [1,2,*]**, Xianming Xiao** [3]**, Jinhao Guo** [1,2]**, Kun He** [1,2] **and Xingzhi Ma** [1,2]

[1] State Key Laboratory for Enhanced Oil Recovery, Beijing 100083, China; jinhao.guo@outlook.com (J.G.); hekun1@petrochina.com.cn (K.H.); maxingzhi@petrochina.com.cn (X.M.)
[2] Research Institute of Petroleum Exploration and Development, PetroChina, Beijing 100083, China
[3] School of Energy Resources, China University of Geosciences, Beijing 100083, China; xmxiao@cugb.edu.cn
[*] Correspondence: jkmi@petrochina.com.cn; Tel.: +86-010-8359-3053

Abstract: The temperature or maturity limit of methane (CH_4) cracking is very useful for the determination of the most depth or the highest maturity in natural gas exploration owing to the composition of over mature gas. In this work, three series of CH_4 cracking experiments were conducted under different conditions of $N_2 + CH_4$, $N_2 + CH_4 +$ montmorillonite and $N_2 + CH_4 +$ shale, respectively, in a gold tube system. The experimental results show that some heavy gas with negative carbon isotope composition could be generated in the three series experiments and that shale has more intense catalysis for CH_4 cracking than montmorillonite. The catalysis of metal elements distributed in the minerals of shale is attributed to CH_4 cracking acceleration. The shale catalysis makes the maturity threshold of CH_4 substantial cracking decrease from 6.0%R_o under no catalysis, to 4.5%R_o under a shale system in a geological setting. Nevertheless, we suggest not to lightly practice natural gas exploration in shale with the maturity range of 3.5–4.5%R_o, as the maturity threshold of gas generation from oil prone organic matter distributed extensively in shale is 3.5%R_o.

Keywords: CH_4 cracking experiment; catalysis; shale; metal element; maturity threshold

1. Introduction

A remarkable geological characteristic in natural gas exploration appears in the 21st century, that is, the maturity level of natural gas source and the depth of natural gas become higher and deeper, respectively. The resources of natural gas found in over-mature shale are increasing in the world [1]. The highest documented maturity of shale gas and the most depth of natural gas reservoir arrive 4.0%R_o and 8000 m according to the data, respectively [2,3]. Consequently, a problem appears, that is, what the highest maturity level for shale or the most depth for natural gas are. The answer to this problem is very significant and will help to increase the success ratio of gas well drilling in over-mature shale, and reduce the cost in gas well drilling.

Another geochemical feature of over mature natural gas is isotopic reversal. Natural gas with the isotopic reversal feature was originally regarded to be of abiogenic origin before shale gas with this feature was determined. The heavy hydrocarbon components in abiogenic gas were generally thought to be caused by the polymerization of CH_4 formed by Fischer–Tropsch synthesis between H_2 and CO_2 (or CO) as well [4–6]. Although much research has studied the mechanism about the isotopic reversal of organic origin gas generated at the over mature stage, but no common knowledge on this problem was obtained. Their observations on the same can be classified into four interpretations. (1) Mixing between primary gas from kerogen decomposition and secondary gas from the cracking of remained hydrocarbons in shale causes the isotopic reversal of shale gas at the over mature stages [2,7–9]. (2) The redox reactions between water and CH_4 at 250–300 °C generated isotopically light carbon dioxide and hydrogen in the over mature phase, which further interacted and formed isotopically light ethane (C_2H_6), and finally caused the isotopic

reversal of shale gas [9,10]. (3) The isotope fractionation mechanism during gas desorption from depressurized late-mature shale leads to isotope reversal of the residual gas (shale gas) [11]. (4) The polymerization occurring in the early stage of CH_4 cracking brings the isotopic abnormal trend of over mature natural gas [12,13]. However, only the last one is feasible in theory and supported by experimental data in the four interpretations. The others might be just speculation or a mathematical model and are not supported by simulation experiment [13].

The theory of oil and gas generation suggests that organic matter would generate oil and gas as it is buried to some depth. With the geological temperature increasing, the oil accumulated in reservoir or remaining in source rock would crack into gas. Natural gas would crack into the ultimate products, carbon and hydrogen, with further geological temperature. Besides geological factors of natural gas preservation, the most depth or maturity for natural gas exploration is attributed to CH_4 stability in a geological setting as it is the main component of natural gas, especially for over mature gas. Mi et al. [13] proposed that the maturity of CH_4 substantial cracking was 6.0%R_o according to geological deduction on the experimental data of CH_4 cracking. However, the highest documented maturity of shale where industrial shale gas reservoir was found was only 4.0%R_o [2]. What is the reason for the difference between the maturity limit of CH_4 substantial cracking from the experiment result (6.0%R_o) and the reported maximum maturity (4.0%R_o) in shale gas exploration practice?

Many experiments have proven that different mineral or geological fluids have various effect on oil cracking [14–17]. Thus, the mineral in shale might affect CH_4 cracking as well. Although thermo-catalytic decomposition of natural gas to produce pure hydrogen production is used extensively in the fuel industry [18], only a few studies on natural gas cracking in a geological setting have been published, especially for CH_4. In this study, three series of CH_4 cracking experiments were conducted under $N_2 + CH_4$ (series 1), $N_2 + CH_4$ + montmorillonite (series 2), and $N_2 + CH_4$ + shale (series 3) system, respectively. The scope of the experiments is to investigate whether or not shale has a catalysis on CH_4 cracking, and further, to determine the maximum maturity limit of CH_4 substantial cracking in a shale system.

2. Sample and Experiment

2.1. Sample

Three series of CH_4 cracking experiments were conducted under the condition of $N_2 + CH_4$ (Series 1), $N_2 + CH_4$ + montmorillonite (Series 2), and $N_2 + CH_4$ + shale (Series 3), respectively. In this experiment, N_2 was selected as the reference gas for the decomposition temperature more than 3000 °C, and it could not crack in the experimental temperature range of 500~800 °C. The gas mixture was purchased from Zhaoge Gas Company, Beijing, China, and the CH_4 and N_2 (v/v) mixing ratio was 89.67% and 10.33%. The value of $\delta^{13}C_1$ was −26.07‰ and no other hydrocarbon gases were detected in the gas mixture by gas chromatography (GC).

Montmorillonite, involved in the series 2 experiment, is commercially available montmorillonite K-10 (MK-10) purchased from ACROS 111 ORGANICS (USA). The shale sample involved in the series 3 experiment was collected from the shale gas reservoir of N218 well, Longmaxi formation deposited in Silurian of Sichuan basin, China. Prior to loading the shale in a tube, the shale sample was crashed below 80 mesh. Then the crashed shale was heated to 800 °C in a gold tube at a heating rate of 20 °C/h and held 2 h at 800 °C to exhaust the potential of gas generation from the organic matter in the shale during the cracking experiment. The geochemistry of original and heated shale is listed in Table 1. According to the equation of $R_o = 0.018 \times Tmax-7.16$ proposed by Jarvie et al. [19], the calculated maturity of original and heated shale is about 2.2%R_o and 4.23%R_o, respectively. This indicates the maturity of the original shale reaches over maturity level and the heated shale has no potential of gas generation. The mineral composition of the original shale

listed in Table 2 was measured by Quemscan. The amount of MK-10 or shale added in the tube was the same, 50 mg in every temperature in the series 2 and 3 experiments.

Table 1. Geochemistry of original and heated shale samples.

Samples	TOC (%)	T_{max} (°C)	S_1 (mg/g)	S_2 (mg/g)	HI (mg/g TOC)
Original shale	1.33	520	0.1	0.31	23.31
Heated shale	1.18	633	0	0	0

Table 2. Mineral composition of the original shale sample.

Mineral	(%)	Mineral	(%)	Mineral	(%)	Mineral	(%)
Quartz	32.31	Albite	3.26	Chlorite	0.93	Kaolinite	0.16
Illite	29.04	Pyrite	3.02	Muscovite	0.34	Rutile	0.16
Biotite	10.81	Gypsum	2.54	Smectite	0.33	Glauconite	0.15
Calcite	6.44	Feldspar	2.33	Siderite	0.26	Others	0.03
Barite	5.63	Dolomite	2.01	Apatite	0.25		

2.2. Experiment

The experiments in this study were conducted in a gold tube system, which is an extensively used experimental equipment for organic matter pyrolysis and oil cracking [13,20]. The length, outer diameter, and thickness of the gold tube used in this experiment are 100, 5.5, and 0.25 mm, respectively. One end of the tube was sealed by argon-arc welding before the gas mixture and solid sample (MK-10 or shale) were loaded. A special device, which could connect a vacuum pump and the open tube mouth, was used in gas mixture loading. Prior to gas mixture injection, the tube was vacuumized via the vacuum pump. Then, the gas mixture was injected into the tube from a gas cylinder. Finally, the tube open end was sealed by argon-arc welding. The tube was immersed in ice water during the welding process. The pressure of gas loaded in the tube, which was monitored using a pressure gauge on the gas cylinder, was approximately 4 atm in this experiment.

The gold tube experiment system had 20 autoclaves. Each autoclave had an independent temperature controller. The fluid pressure in autoclave and heating process of each autoclave could be controlled by a computer. All autoclaves were kept a constant fluid pressure of 50 MPa during experiment. The heating program of the autoclave with the tube in this experiment was as follows: heated first from 20 °C to 300 °C in 1 h and held for 30 min, then heated at a heating rate of 20 °C/h to the target temperature. The autoclave heating was stopped after the target temperature was reached. The tubes were moved for analysis as autoclave cooled naturally to room temperature.

Two gold tubes were used for each temperature experiment in case of breakage. Another objective of additional tubes used were as replicates for gas analysis.

The composition analysis of the original gas mixture and the gas produced at different temperatures in this experiment was carried out on Wasson-Agilent 7890 series GC. The heating program for the GC oven was as follows: heating started from an initial temperature of 68 °C (isothermal held for 7 min), then heated to 90 °C (at a rate of 10 °C/min and then held isothermal for 1.5 min), finally to 175 °C (at a rate of 15 °C/min and then held isothermal for 1.5 min). An external standards method was employed for the chromatographic calibration using a reference gas mixture of H_2, O_2, N_2, CO_2, H_2S, CH_4, C_2H_6, C_3H_8, iC_4H_{10}, nC_4H_{10}, iC_5H_{12}, and nC_5H_{12}. Certified gas standards were prepared at a precision less than ±0.1 mol% for each component made by BAPB Inc., New Berlin, WI, USA.

The carbon Isotopic composition of hydrocarbon gases measurements were conducted on an Isochrom II GC-IRMS coupled with a Poraplot Q column. The heating started from an initial temperature at 30 °C (isothermal for 3 min). Then, heated at a heating rate of 15 °C/min to 150 °C (isothermal for 8 min). The $\delta^{13}C$ analysis for each hydrocarbon gas was repeated at least twice to ensure the analytical error of each component less than 0.5‰.

3. Experiment Results

3.1. Gas Components

The composition of gas produced at different temperatures in three series CH_4 cracking experiments are summarized in Table 3. Besides the CH_4 and N_2 in original gas mixture, several heavy hydrocarbon gases (including alkane and alkene) and H_2 were formed during three series experiments, at different temperatures. CH_4 concentration decreased generally with increasing temperature, and the decreasing could be divided into two segments (a slow and a steep decreasing) in three series experiments (Figure 1a). The inflexion temperatures corresponding to an obvious decrease in CH_4 concentration were 700 °C, 675 °C, and 650 °C, respectively, in series 1, 2, and 3 experiments. The reductions in CH_4 concentration at the highest experimental temperature of 800 °C were 6.36%, 7.48%, and 9.42%, respectively, in series 1, 2, and 3 experiments. Both the concentration t of C_2H_6, the highest newly formed hydrocarbon component, and that of other heavy gases increased at relatively low temperature and then decreased with increasing temperature (Figure 1b and Table 3). The highest total concentrations of heavy gas (C_2–C_5) were 1.04%, 0.53%, and 0.46% in series 1, 2, and 3 experiments, respectively. The total concentration of heavy gas decreased to 0.72%, 0.37%, and 0.21% at the highest experimental temperature (800 °C) in series 1, 2, and 3 experiments, respectively. The temperatures at which the concentrations of heavy gas reached their maximums were 750 °C, 725 °C, and 725 °C in series 1, 2, and 3 experiments, respectively. Although H_2 concentration increased with increasing temperature in three series experiments, the highest concentrations of H_2 were different, 0.88%, 2.66%, and 4.49% (Figure 1c and Table 3). The corresponding temperatures at which H_2 concentration increased obviously were different as well. They were 700 °C, 675 °C, and 650 °C in series 1, 2, and 3 experiments, respectively.

3.2. Carbon Isotopic Composition of Hydrocarbon Gas

The carbon isotopic composition of hydrocarbon gas at different temperatures of the three series experiments is presented in Table 4. The values of $\delta^{13}C_1$ generally increased with increasing temperature in three series CH_4 cracking experiments (Figure 2). Although the variations $\delta^{13}C_1$ in three series experiments could be divided into two segments, a slow increasing segment and a rapid one, the temperature inflexions corresponding to $\delta^{13}C_1$ values becoming big obviously were different, 650 °C, 675 °C, and 700 °C in the three series experiments, respectively. The $\delta^{13}C_1$ values at the highest experimental temperature of the three series experiments were $-24.60‰$, $-23.31‰$, and $-21.95‰$, respectively.
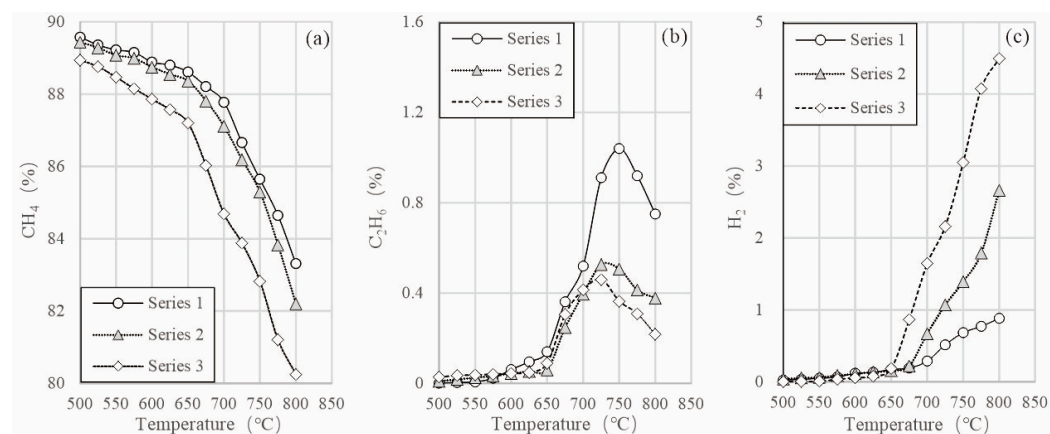

Figure 1. Concentration variation of different gas components with increasing temperature in three series experiments. (**a**) Concentration variation of CH_4 with increasing experimental temperature. (**b**) Concentration variation of C_2H_6 with increasing experimental temperature. (**c**) Concentration variation of H_2 with increasing experimental temperature.

Table 3. Gas components generated under different temperatures in three series CH_4 cracking experiments.

Series	Temp (°C)	Components (%)								
		H_2	CH_4	C_2H_6	C_3H_8 ($\times 10^{-1}$)	C_2H_4 ($\times 10^{-3}$)	C_3H_6 ($\times 10^{-3}$)	iC_4 ($\times 10^{-3}$)	nC_4 ($\times 10^{-3}$)	N_2
1	500	0.03	89.58	0.00	0.01	0.00	0.00	0.00	0.00	10.39
	525	0.03	89.36	0.00	0.03	0.00	0.00	0.00	0.16	10.60
	550	0.05	89.23	0.00	0.04	0.00	0.09	0.24	0.60	10.72
	575	0.07	89.16	0.02	0.07	0.00	0.22	0.16	0.27	10.76
	600	0.12	88.89	0.04	0.21	0.00	0.58	0.28	0.37	10.93
	625	0.13	88.80	0.07	0.24	0.12	2.18	0.39	0.44	10.97
	650	0.17	88.62	0.11	0.28	0.93	1.59	1.48	1.10	11.07
	675	0.19	88.22	0.31	0.47	1.78	1.23	1.65	2.11	11.23
	700	0.29	87.78	0.48	0.35	1.08	0.93	0.87	1.24	11.41
	725	0.51	86.66	0.88	0.27	0.90	0.63	0.57	0.74	11.91
	750	0.68	85.65	1.01	0.26	0.89	0.57	0.56	0.68	12.63
	775	0.77	84.65	0.89	0.26	0.85	0.60	0.54	0.58	13.66
	800	0.88	83.31	0.72	0.25	0.61	0.27	0.51	0.53	15.06
2	500	0.04	89.44	0.01	0.00	0.00	0.00	0.00	0.00	10.51
	525	0.05	89.28	0.02	0.01	0.00	0.00	0.00	0.00	10.65
	550	0.06	89.08	0.02	0.01	0.00	0.00	0.00	0.00	10.84
	575	0.09	88.99	0.03	0.02	0.00	0.00	0.00	0.05	10.89
	600	0.11	88.75	0.04	0.02	0.00	0.00	0.00	0.17	11.10
	625	0.13	88.55	0.05	0.04	0.00	0.00	0.16	0.23	11.27
	650	0.15	88.36	0.06	0.03	0.01	0.00	0.15	0.26	11.42
	675	0.22	87.91	0.24	0.11	0.25	0.12	0.33	0.56	11.62
	700	0.67	87.11	0.38	0.11	0.78	0.14	0.30	0.32	11.82
	725	1.07	86.19	0.51	0.11	0.23	0.11	0.00	0.26	12.22
	750	1.39	85.09	0.50	0.08	0.00	0.00	0.00	0.17	13.01
	775	1.79	83.83	0.41	0.08	0.00	0.00	0.00	0.15	13.96
	800	2.66	82.19	0.37	0.04	0.00	0.00	0.00	0.00	14.78
3	500	0.00	88.94	0.03	0.01	0.00	0.00	0.00	0.00	11.03
	525	0.00	88.76	0.03	0.03	0.00	0.00	0.23	0.34	11.19
	550	0.01	88.47	0.04	0.03	0.00	0.00	0.20	0.26	11.48
	575	0.03	88.16	0.04	0.03	0.00	0.00	0.17	0.32	11.77
	600	0.06	87.86	0.04	0.04	0.00	0.00	0.17	0.26	12.03
	625	0.07	87.58	0.04	0.04	0.00	0.00	0.17	0.21	12.30
	650	0.19	87.20	0.08	0.06	0.11	0.09	0.15	0.22	12.52
	675	0.86	86.03	0.30	0.07	0.22	0.12	0.00	0.13	12.80
	700	1.64	84.69	0.41	0.07	0.00	0.00	0.00	0.00	13.25
	725	2.16	83.88	0.45	0.05	0.00	0.00	0.00	0.00	13.50
	750	3.05	82.82	0.36	0.04	0.00	0.00	0.00	0.00	13.76
	775	4.07	81.21	0.31	0.03	0.00	0.00	0.00	0.00	14.41
	800	4.49	80.25	0.21	0.03	0.00	0.00	0.00	0.00	15.04

Series 1: $N_2 + CH_4$; Series 2: $N_2 + CH_4$ + MK-10; Series 3: $N_2 + CH_4$ + shale.

Table 4. Carbon isotopic composition of CH_4 and C_2H_6 at different temperatures in three series experiments.

Temperature (°C)	$\delta^{13}C$(‰)					
	Series 1		Series 2		Series3	
	C_1	C_2	C_1	C_2	C_1	C_2
500	−25.71		−25.83		−25.88	
525	−25.71		−25.74	−34.85	−25.84	−34.62
550	−25.84		−25.68	−34.83	−25.75	−34.65
575	−25.84	−33.22	−25.71	−34.81	−25.51	−34.58
600	−26.01	−32.74	−25.67	−34.94	−25.38	−34.55
625	−25.91	−32.47	−25.66	−34.89	−25.26	−34.52
650	−25.97	−30.26	−25.56	−34.61	−25.13	−32.07
675	−25.81	−27.47	−25.52	−29.85	−24.48	−26.42
700	−25.83	−26.02	−25.11	−28.15	−23.92	−24.63
725	−25.66	−25.31	−24.86	−25.91	−23.14	−23.88
750	−25.28	−24.82	−24.43	−25.56	−22.69	−22.32
775	−25.04	−24.68	−23.86	−24.46	−22.29	−21.85
800	−24.60	−24.50	−23.31	−23.29	−21.95	−21.66

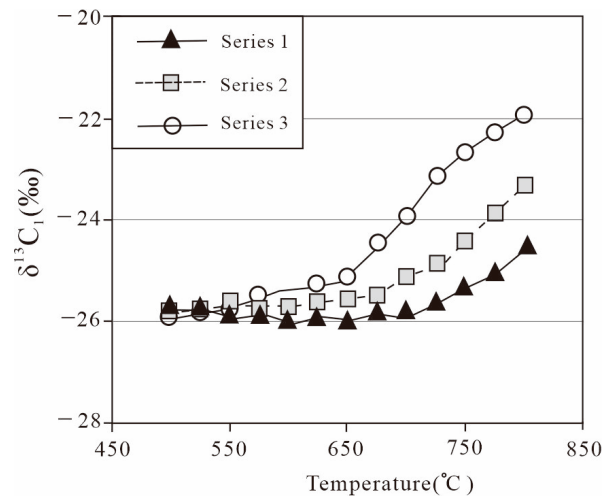**Figure 2.** Variation of $\delta^{13}C_1$ with increasing temperature three series experiments.

Similar to the $\delta^{13}C_1$ variation with increasing experimental temperature in the three series experiments, $\delta^{13}C_2$ also increased generally with increasing temperature (Figure 3). The $\delta^{13}C_2$ variation with increasing temperature could be classified into three segments, a gradual increase or no increase, a rapid one, and a slow one in three series experiments. There was only a little variation in $\delta^{13}C_2$ (0.75‰) in the first segment of the series 1 experiment. Hardly any variation in $\delta^{13}C_2$ was observed in the first segment of the series 2 and 3 experiments. The temperature inflexions corresponding to the first segment to the second segment were different, 625 °C, 650 °C, and 625 °C in the three series experiments, respectively. The temperature inflexions corresponding to the second segment to the third segment were the same, 725 °C in the three series experiments.
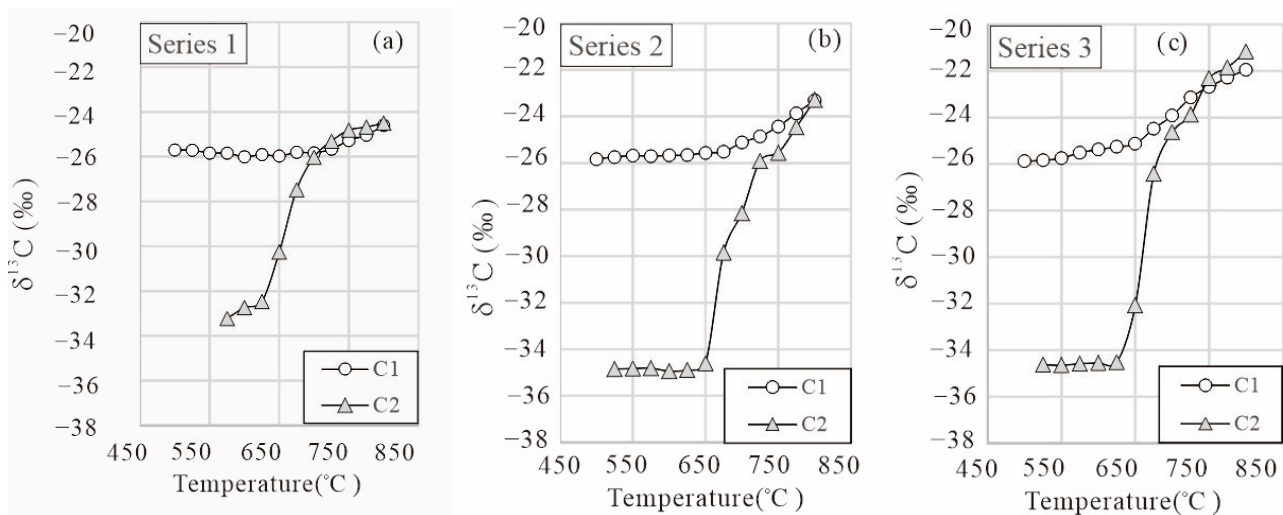
Figure 3. Variation of $\delta^{13}C_1$ and $\delta^{13}C_2$ with increasing temperature three series experiments. (**a**) Variation of $\delta^{13}C_1$ and $\delta^{13}C_2$ with increasing temperature in series 1 experiment. (**b**) Variation of $\delta^{13}C_1$ and $\delta^{13}C_2$ with increasing temperature in series 2 experiment. (**c**) Variation of $\delta^{13}C_1$ and $\delta^{13}C_2$ with increasing temperature in series 3 experiment.

In the series 1 experiments, the distribution between $\delta^{13}C_1$ and $\delta^{13}C_2$ turned from a reversal trend ($\delta^{13}C_1 > \delta^{13}C_2$) to a normal one ($\delta^{13}C_1 < \delta^{13}C_2$) above 700 °C. The distribution between $\delta^{13}C_1$ and $\delta^{13}C_2$ kept an abnormal trend in the whole temperature range in the series 2 and 3 experiments. Nevertheless, the difference between $\delta^{13}C_1$ and $\delta^{13}C_2$ in the three series experiments became less with increasing temperature, and finally tended to be equal at 800 °C.

3.3. Solid Products

The inner walls photo of the tubes heated to different temperatures are shown in Figure 4. In the three series experiments, the color of inner walls turned from gold into brown, and finally into dark. The corresponding temperature at which the color of inner walls turned from gold into brown were 725 °C, 700 °C and 675 °C, respectively, in series 1, series 2, and series 3 experiments.
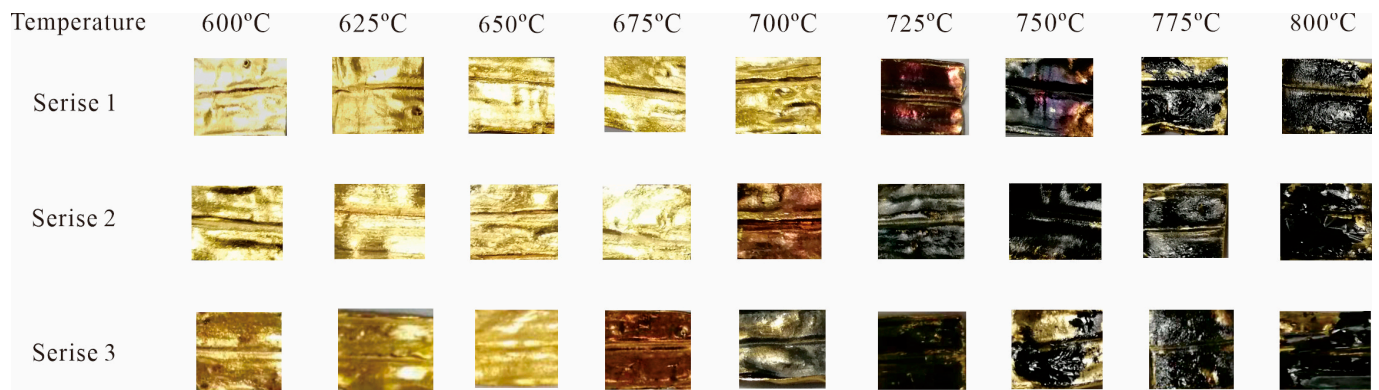

Figure 4. The inner walls photo of the tubes heated to different temperatures in three series experiments.

Some black particles could be observed in the residual MK-10 heated above 700 °C in series 2 experiments by scanning electron microscope. The black particles and the black film on the tube inner wall were identified as solid carbon by Energy Dispersive X-ray Spectroscopy (EDS) analysis (Figure 5). Moreover, the color of the solid residues became dark gradually with increasing temperature in the series 2 experiment (Figure 6). The corresponding temperature at which the color of solid residues became obviously dark in the series 2 experiment was 700 °C. This was consistent with the temperature at which the color of the inner walls became brown in the series 2 experiment (Figure 4). Some black particles were observed in solid residues heated to different temperature as well in the series 3 experiment. However, these black particles in shale residues were not distinguished to be the newly formed carbon particles or the organic matter particles originally existing in the shale.
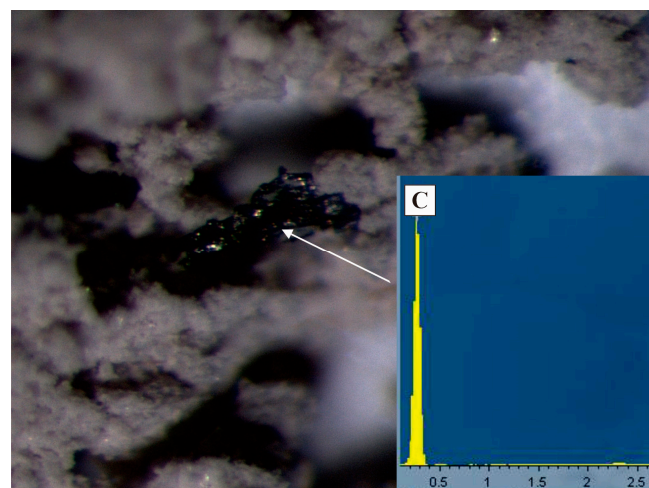

Figure 5. Black particles in solid residue and the energy dispersive spectrum in series 2 experiment at 750 °C.
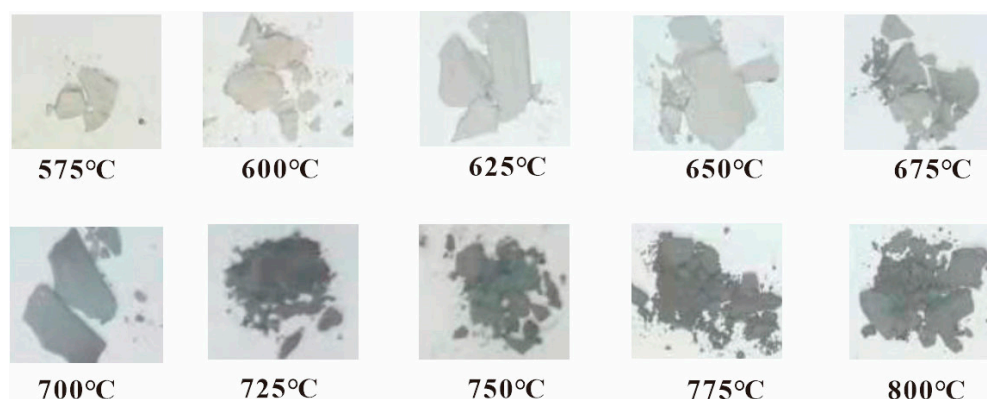
Figure 6. Color variation of solid residues with temperature increasing in series 2 experiment.
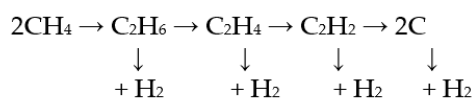
4. Discussion

4.1. Process of CH₄ Cracking

The variation of CH_4 concentration with increasing temperature presented in Figure 1 shows that it could be divided into two stages, a slow decreasing stage and a rapid one (Figure 1a). The two stages variation of CH_4 concentration is consistent with that of H_2 (Figure 1c) and that of $\delta^{13}C_1$ (Figure 2). This indicates CH_4 cracking could generally be divided into two steps, early cracking and substantial cracking. In the substantial cracking stage, CH_4 concentration would decrease obviously. In three series experiments, the temperatures corresponding to an obvious decrease in CH_4 concentration were 700 °C, 675 °C, and 650 °C, respectively (Figure 1a). This indicates that montmorillonite and shale could accelerate CH_4 cracking, and shale has more intense catalysis for CH_4 cracking. Shale acceleration on CH_4 cracking also embodies the highest H_2 concentration (Figure 1c) and the biggest $\delta^{13}C_1$ values (Figure 2) at the highest experimental temperature (800 °C) in the three series experiments.

Much research indicated that the formation of higher carbon number hydrocarbons during the CH_4 cracking process followed the mechanism of free radical reaction [20,21]. In early cracking, CH_4 crack into $CH_3\bullet$ radicals and protons first. $CH_3\bullet$ radicals would combine and form heavy gas with H_2 formation by protons combing. This process of heavy gas formation could be viewed as CH_4 polymerization. There are two kinds of CH_4 molecules in original reactants, $^{12}CH_4$ and $^{13}CH_4$. The ^{12}C–H bonds are more chemically active than ^{13}C–H [21–23]. The ^{12}C–H bond in the CH_4 molecule would cleavage preferentially than the ^{13}C–H bond during the CH_4 cracking process. Thus, the produced $CH_3\bullet$ is depleted in ^{13}C, while residual CH_4 is enriched in ^{13}C. The newly formed H^+ would combine and form H_2 during the CH_4 cracking process. The $CH_3\bullet$ depleted in ^{13}C also combine and form C_2H_6 depleted in ^{13}C. Thus, the carbon isotopic reversal (Figure 3) of hydrocarbon gas generated in CH_4 cracking is reasonable.

The temperatures at wihch CH_4 concentration obviously decreased are 700 °C, 675 °C, and 650 °C in the three series experiments (Figure 1a), respectively. These are lower than that of solid carbon appearance at 725 °C, 700 °C, and 675 °C (Figure 4) in the three series experiments. The seeming conflict phenomenon just is evidence that solid carbon formation happened after CH_4 substantial cracking.

CH_4 cracking is a stepwise dehydrogenation process and the overall reaction of CH_4 cracking involves the following steps at high temperatures [24]:

$$2CH_4 \rightarrow C_2H_6 \rightarrow C_2H_4 \rightarrow C_2H_2 \rightarrow 2C$$
$$\downarrow \quad\quad \downarrow \quad\quad \downarrow \quad\quad \downarrow$$
$$+ H_2 \quad + H_2 \quad + H_2 \quad + H_2$$

In other words, the overall process of CH_4 cracking could be divided into two steps, heavy gas formation vs. $CH_3\bullet$ groups combination and solid carbon formation by heavy gas further dehydrogenation. The first step could be viewed as CH_4 polymerization [13].

The second one is a relatively complex process which involves the dehydrogenation of heavy gas (alkane and alkene gas) and the formation of solid carbon. The conversion from heavy gas to single carbon still needs several steps of dehydrogenation. Alkane and alkene heavy components measured in the gaseous products in the three series experiments (Table 3) is firm evidence of the aforementioned mechanism of CH_4 cracking.

When CH_4 cracking has entered into the substantial cracking stage in the three experiments, the concentration of C_2H_6 increases continuously (Figure 1). For example, when CH_4 concentration decreases obviously above 700 °C, the C_2H_6 concentration just arrives the maximum at 750 °C. This seems to conflict with the general knowledge in chemistry that the thermal stability of C_2H_6 is lower than that of CH_4. The result does not mean that the thermal stability of C_2H_6 is higher than that of CH_4, but that the ratio of C_2H_6 formation by CH_4 polymerization is greater than that of C_2H_6 further dehydrogenation in the temperature range at which CH_4 concentration decreases obviously, accompanying heavy gas concentration increasing. This experimental result could also be explained by the hypothesis proposed by Xia and Gao [21] that heavy gas cracking and generation is a partly reversible reaction at high temperatures. Shuai et al. [25] proved that the generation and cracking of C_2H_6 could co-exist at high temperatures by a coal pyrolysis experiment in a gold tube system. Our experiment indicates that the heavy gas (alkane gas and alkene gas) is just an intermediate product during the CH_4 cracking process. Thus, heavy gas could not disappear completely as long as CH_4 did not crack into solid carbon entirely.

4.2. Primary Study on Shale Acceleration Mechanism for CH_4 Cracking

Hydrogen is a very clear energy and is used extensively in the fuel industry, especially in space technologies in the last two decades. However, hydrogen is not a primary energy source, and is generally produced from other resources. The thermo-catalytic decomposition of CH_4 can be regarded as a cornerstone for pure hydrogen production [26]. In the process of industrial production of hydrogen by CH_4 cracking, a wide variety of transition metals (Fe, Al, Co, Ni, Cu, etc.) and silicon dioxide were selected as catalysts to increase the conversion of CH_4 to hydrogen [26–28]. Our experimental result shows that both montmorillonite and shale would promote CH_4 cracking. Shale presents a more intense acceleration on CH_4 cracking than montmorillonite. Montmorillonite is a silicate mineral bearing several metal elements (Na, Ca, Al, Mg, Fe). Thus, it is reasonable that montmorillonite promotes CH_4 cracking. It is well known that shale is a fine-grained sedimentary rock. Generally, the mineral composition of shale includes clay (montmorillonite, kaolinite, and illite, etc.), detrital mineral (quartz, feldspar, and pyrite, etc.), and some organic matter. All the clay minerals are metal-bearing silicate minerals. The metal in clay minerals of shale would also accelerate the CH_4 cracking. Chen et al. [12] proved that shale could increase CH_4 conversion above 580 °C by 72 h isothermal experiment conducted in a gold tube system. The analysis result shown in Table 2 indicates that the shale involved in the series 3 experiment bears a complex mineral composition. Besides clay minerals, several detrital minerals bearing metal (siderite, pyrite, etc.) distribute in the shale. The metal elements in detrital minerals might also promote CH_4 cracking. This might be the reason that shale has a more intense acceleration on CH_4 cracking than montmorillonite. Although the experiments in this study could not prove which kinds of metals in shale are the main operator to accelerate CH_4 cracking, it is confessed that the metal distributed in different minerals of shale accelerates CH_4 cracking.

It is well known that the function of a catalyst is to decrease reaction activation energy. Just as catalysis of montmorillonite and shale, the lowest temperature at which heavy gas, the intermediate product of CH_4 cracking, could be measured by Wasson-Agilent 7890 GC in the series 2 and 3 experiments (500 °C) is lower than that in the series 1 experiment (575 °C, Table 3). However, the highest concentrations of heavy gas in the series 2 and 3 experiments are lower than that in the series 1 experiment (Table 3, and in Figure 1b). The above variation of heavy gases concentration in the three series experiment indicates that metal elements in montmorillonite and shale might accelerate

each step of dehydrogenation during the whole CH_4 cracking process. Although the metal catalysis on CH_4 polymerization would cause the heavy gas concentration increase, the more intense catalysis on dehydrogenation of heavy gases might be attributed to the lower concentrations of heavy gases in the series 2 and 3 experiments, compared with that in the series 1 experiment. The greater decrease in CH_4 concentration and the more H_2 generation (Figure 1c), as well as the heavier value of $\delta^{13}C_1$ (Figure 2) in the series 2 and 3 experiments indicate that both montmorillonite and shale could accelerate CH_4 cracking. Moreover, shale bears more acceleration on CH_4 cracking than montmorillonite.

4.3. Geological Significance of the Experiments

Our experimental result indicates that shale has more intense acceleration on CH_4 cracking than that of MK-10. The final objective of our experiments is to determine the maturity limit of CH_4 cracking under a shale system and to provide some reference for shale gas exploration. Therefore, the experimental temperature should be converted to actual geological temperature or maturity (R_o). Mi et al. [29] proposed a formula to convert experimental temperature to R_o according to a coal pyrolysis experiment, which was conducted at the same experimental conditions as our experiment. The relationship between R_o and the experimental temperature is described in Equation (1).

$$R_o = 0.114 \times \exp{(0.00563 \times T)} + 0.056 \tag{1}$$

(T, experiment temperature/°C)

The experiment result shows that the temperatures corresponding to CH_4 substantial cracking are 650 °C, 675 °C, and 700 °C, respectively, under $N_2 + CH_4$, $N_2 + CH_4 + MK-10$ and $N_2 + CH_4 +$ shale condition. The maturity levels corresponding to the three temperatures are 4.48%R_o, 5.15%R_o, and 5.92%R_o according to Equation (1). Thus, the maturity limit of CH_4 substantial cracking is 4.48%R_o in a shale system. This limit of CH_4 substantial cracking is slightly higher than the reported maximum maturity level of 4.0%R_o in shale gas exploration [2,11]. This is attributed to the upper maturity limit of gas generation from shale being 3.5%R_o [20]. The natural gas stored in shale with maturity above 3.5%R_o would lose easily to exhaustion during very long geological history, for no gas would continuously supply from the shale. Therefore, we suggest that great care should be taken to explore natural gas in shale with maturity above 3.5%R_o.

5. Conclusions

In this work, three series cracking experiments of an N_2 and CH_4 mixture gas, a mixture gas with montmorillonite, and a mixture gas with shale powder, respectively, were conducted in a gold tube system. The experimental results show that both montmorillonite and shale could accelerate CH_4 cracking, and that shale has more intense catalysis on CH_4 cracking. Some hydrocarbon heavy gas could be generated during the CH_4 cracking process. The heavy alkane gases form by combination of methyl formed in the early CH_4 cracking stage. The unsaturated heavy gases are formed by further dehydrogenation of heavy gas. The combination of methyl with depleted in ^{13}C and formed in CH_4 early cracking is attributed to ^{13}C depletion of heavy gas and carbon isotopic reversal of over mature shale gas. The experimental results also indicate that the heavy gases are intermediate products of CH_4 cracking. Thus, heavy gases could not disappear completely as long as CH_4 did not crack entirely. The catalysis of the metal element distributed in clay and other metalliferous detrital minerals of shale accelerate CH_4 cracking. The geological reckoning of the experimental result suggests that the maturity threshold for substantial CH_4 cracking is about 4.5%R_o under a shale system in a geological setting. Nevertheless, we suggest not to lightly practice natural gas exploration in shale with the maturity space of 3.5–4.5%R_o, as the maturity threshold of gas generation by oil prone organic matter distributed extensively in shale is 3.5%R_o.

References

1. McGlade, C.; Speirs, J.; Sorrell, S. Unconventional gas—A review of regional and global resource estimates. *Energy* **2013**, *55*, 571–584. [CrossRef]
2. Hao, F.; Zou, H. Cause of shale gas geochemical anomalies and mechanisms for gas enrichment and depletion in high-maturity shales. *Mar. Pet. Geol.* **2013**, *44*, 1–12. [CrossRef]
3. Wang, X.L.; He, X.P.; Liu, X.F.; Cheng, T.H.; Li, R.L.; Fu, Q. Key Drilling Technologies for Complex Ultra-Deep Wells in the Tarim Keshen 9 Gas Field (in Chinese with English abstract). *Pet. Drill. Tech.* **2020**, *48*, 15–20.
4. Hu, G.X.; Quyang, Z.Y.; Wang, X.; Wen, Q.B. Carbon isotopic fractionation in the process of Fisher-Tropsch reaction in primitive solar nebula. *Sci. China (Ser. D)* **1998**, *41*, 202–207. [CrossRef]
5. Horita, J.; Berndt, M.E. Abiogenic CH4 formation and isotopic fractionation under hydrothermal conditions. *Science* **1999**, *285*, 1055–1057. [CrossRef]
6. Lollar, B.S.; Lacrampe-Couloume, G.; Voglesonger, K.; Onstott, T.; Pratt, L.; Slater, G. Isotopic signatures of CH_4 and higher hydrocarbon gases from Precambrian Shield sites: A model for abiogenic polymerization of hydrocarbons. *Geochim. Cosmochim. Acta* **2008**, *72*, 4778–4795. [CrossRef]
7. Tilley, B.; Muehlenbachs, K. Isotope reversals and universal stages and trends of gas maturation in sealed, self-contained petroleum systems. *Chem. Geol.* **2013**, *339*, 194–204. [CrossRef]
8. Xia, X.; Chen, J.; Braun, R.; Tang, Y. Isotopic reversals with respect to maturity trends due to mixing of primary and secondary products in source rocks. *Chem. Geol.* **2013**, *339*, 205–212. [CrossRef]
9. Burruss, R.C.; Laughrey, C.D. Carbon and hydrogen isotopic reversals in deep basin gas: Evidence for limits to the stability of hydrocarbons. *Org. Geochem.* **2010**, *42*, 1285–1296. [CrossRef]
10. Zumberge, J.; Ferworn, K.; Brown, S. Isotopic reversal ('rollover') in shale gases produced from the Mississippian Barnett and Fayetteville formations. *Mar. Pet. Geol.* **2012**, *31*, 43–52. [CrossRef]
11. Milkov, A.V.; Faiz, M.; Etiope, G. Geochemistry of shale gases from around the world: Composition, origins, isotope reversals and rollovers, and implications for the exploration of shale plays. *Org. Geochem.* **2020**, *143*, 103997. [CrossRef]
12. Chen, B.; Xu, J.B.; Deng, Q.; Liao, Z.W.; Wang, Y.P.; Faboya, O.L.; Li, S.D.; Liu, J.Z.; Peng, P.A. CH_4 cracking within shale rocks: A new explanation for carbon isotope reversal of shale gas. *Mar. Pet. Geol.* **2020**, *121*, 104591. [CrossRef]
13. Mi, J.K.; He, K.; Shuai, Y.H.; Guo, J.H. Combination of methyl from CH_4 early cracking: A possible mechanism for carbon isotopic reversal of over-mature natural gas. *Geofluids* **2022**, *2022*, 9965046. [CrossRef]
14. Lewan, M. Experiments on the role of water in petroleum formation. *Geochim. Cosmochim. Acta* **1997**, *61*, 3691–3723. [CrossRef]
15. Seewald, J.S. Organic–inorganic interactions in petroleum-producing sedimentary basins. *Nature* **2003**, *426*, 327–333. [CrossRef]
16. Pan, C.; Jiang, L.; Liu, J.; Zhang, S.; Zhu, G. The effects of calcite and montmorillonite on oil cracking in confined pyrolysis experiments. *Org. Geochem.* **2010**, *41*, 611–626. [CrossRef]
17. He, K.; Shuai, Y.H.; Mi, J.K.; Ma, Q.S.; Tang, Y.C.; Fang, Y. Experimental and theoretical studies on kinetics for thermochemical sulfate reduction of oil, C2–5 and methane. *J. Anal. Appl. Pyrolysis* **2019**, *139*, 59–72. [CrossRef]
18. Parolin, G.; Borgogna, A.; Iaquaniello, G.; Salladini, A.; Cerbelli, S. Deactivation-induced dynamics of the reaction front in a fixed-bed catalytic membrane reactor: CH_4 cracking as a case study. *Int. J. Hydrogen Energy* **2020**, *46*, 20159–20170. [CrossRef]
19. Jarvie, D.M.; Claxton, B.L.; Henk, F.; Breyer, J.T. Oil and shale gas from the Barnett Shale, 299 Fort Worth basin, Texas. *AAPG Annu. Meet. Progr.* **2001**, *10*, A100.
20. Mi, J.K.; Zhang, S.C.; Su, J.; He, K.; Zhang, B.; Tian, H.; Li, X.Q. The upper thermal maturity limit of primary gas generated from marine organic matters. *Mar. Pet. Geol.* **2018**, *89*, 120–129. [CrossRef]
21. Xia, X.; Gao, Y. Depletion of 13C in residual ethane and propane during thermal decomposition in sedimentary basins. *Org. Geochem.* **2018**, *125*, 121–128. [CrossRef]
22. Lorant, F.; Prinzhofer, A.; Behar, F.; Huc, A.-Y. Carbon isotopic and molecular constraints on the formation and the expulsion of thermogenic hydrocarbon gases. *Chem. Geol.* **1998**, *147*, 249–264. [CrossRef]
23. Tang, Y.; Perry, J.; Jenden, P.; Schoell, M. Mathematical modeling of stable carbon isotope ratios in natural gases. *Geochim. Cosmochim. Acta* **2000**, *64*, 2673–2687. [CrossRef]
24. Karakaya, C.; Zhu, H.Y.; Loebick, C.; Weissman, J.G.; Kee, R.J. A detailed reaction mechanism for oxidative coupling of CH_4 over $Mn/Na_2WO_4/SiO_2$ catalyst for non-isothermal conditions. *Catal. Today* **2018**, *312*, 10–22. [CrossRef]

25. Shuai, Y.; Peng, P.; Zou, Y.-R.; Zhang, S. Kinetic modeling of individual gaseous component formed from coal in a confined system. *Org. Geochem.* **2006**, *37*, 932–943. [CrossRef]

26. Choudhary, T.V.; Aksoylu, E.; Goodman, D.W. Nonoxidative activation of CH$_4$. *Catal. Rev.* **2003**, *45*, 151–203. [CrossRef]

27. Lunsford, J.H. Catalytic conversion of CH$_4$ to more useful chemicals and fuels: A challenge for the 21st century. *Catal. Today* **2000**, *63*, 165–174. [CrossRef]

28. Li, Y.D.; Li, D.X.; Wang, G.W. CH$_4$ decomposition to COx-free hydrogen and nano-carbon material on group 8–10 base metal catalysts: A review. *Catal. Today* **2011**, *162*, 1–48. [CrossRef]

29. Mi, J.K.; He, K.; Hu, G.Y. *Experiment Technology of Hydrocarbon Generation-Expulsion and Its Application*; Petroleum Industry Press: Beijing, China, 2021; p. 33.